



Three-Dimensional Thermal and Structural Analysis of the First Wall in the SIRIUS-P Reactor

E.A. Mogahed

June 1994

UWFDM-955

Prepared for the Eleventh Topical Meeting on the Technology of Fusion Energy, June 19–23, 1994, New Orleans LA.

FUSION TECHNOLOGY INSTITUTE

UNIVERSITY OF WISCONSIN

MADISON WISCONSIN

DISCLAIMER

This report was prepared as an account of work sponsored by an agency of the United States Government. Neither the United States Government, nor any agency thereof, nor any of their employees, makes any warranty, express or implied, or assumes any legal liability or responsibility for the accuracy, completeness, or usefulness of any information, apparatus, product, or process disclosed, or represents that its use would not infringe privately owned rights. Reference herein to any specific commercial product, process, or service by trade name, trademark, manufacturer, or otherwise, does not necessarily constitute or imply its endorsement, recommendation, or favoring by the United States Government or any agency thereof. The views and opinions of authors expressed herein do not necessarily state or reflect those of the United States Government or any agency thereof.

**Three-Dimensional Thermal and Structural
Analysis of the First Wall in the SIRIUS-P
Reactor**

E.A. Mogahed

Fusion Technology Institute
University of Wisconsin
1500 Engineering Drive
Madison, WI 53706

<http://fti.neep.wisc.edu>

June 1994

UWFDM-955

Prepared for the Eleventh Topical Meeting on the Technology of Fusion Energy, June 19–23, 1994,
New Orleans LA.

THREE-DIMENSIONAL THERMAL AND STRUCTURAL ANALYSIS OF THE FIRST WALL IN THE SIRIUS-P REACTOR

Elsayed A. Mogahed
Fusion Technology Institute, University of Wisconsin-Madison
1500 Johnson Drive
Madison, WI 53706-1687
(608) 263-6398

ABSTRACT

The thermal-structural behavior and performance of the SIRIUS-P power reactor first wall concept is analyzed. The SIRIUS-P conceptual design study is of a 1.0 GWe laser driven inertial confinement fusion power reactor utilizing near symmetric illumination of direct drive targets. Sixty laser beams providing a total of 3.4 MJ of energy are used at a repetition rate of 6.7 Hz with a nominal target gain of 118. The spherical chamber has an internal radius of 6.5 m and consists of a first wall assembly made from carbon-carbon composite material, and a blanket assembly made of SiC composite material. The chamber is cooled by a flowing granular bed of solid ceramic materials, non-breeding TiO_2 for the first wall assembly and breeding Li_2O for the blanket assembly. Helium gas ($P = 0.15$ MPa) is used in a fluidized bed outside the reactor to return the particles to the top of the reactor. A moving bed is chosen over a fluidized bed because of its superior heat transfer capability. The heat transfer in a moving bed depends on the level of agitation and on the effective thermal conductivity of the solid material and the interstitial gas, whereas in a fluidized bed, it is entirely dominated by the thermal conductivity of the carrier gas. This work describes the three-dimensional thermo-structural steady state analysis of the first wall coolant tubes. The performance of the first wall depends, under normal operating conditions, on the thermal loading conditions and internal coolant pressure loading conditions. The analysis utilizes a commercial finite element analysis code with complete 3-D modeling. The analysis shows that the stresses are dominated by bending due to the internal pressure of the He gas; modifying the shape of the tube from purely elliptical at the midplane, while keeping the flow area constant, reduces the stresses. A

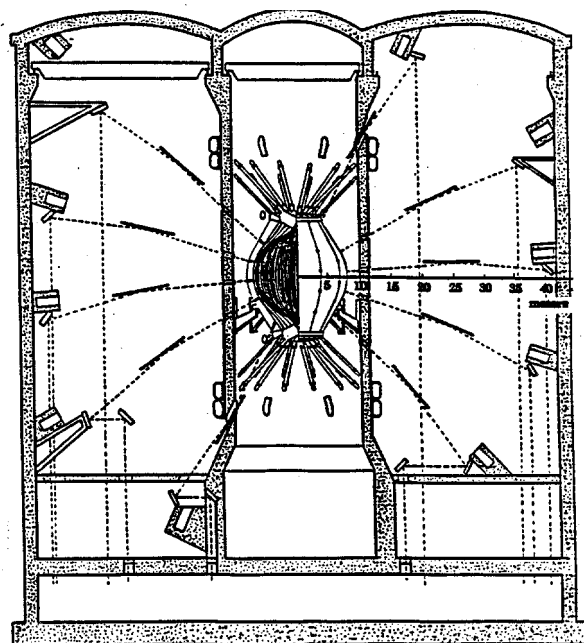


Fig. 1. SIRIUS-P reactor building showing the laser beams and the reactor cavity.

comparison between the results of this 3-D model with a previous 2-D study shows a pronounced effect on the temperature distribution. On the other hand, the 3-D model has a smaller effect on the stress distribution. In general the design examined is shown to be capable of withstanding the loading conditions imposed, although the effect of such factors as pulsed or partially loaded operation should be carefully examined.

I. INTRODUCTION

SIRIUS-P (Fig. 1) has a unique first wall cooling system design. The first wall assembly consists of 12 modules, each with an equal number of tubes which cover the spherical shape of the chamber from top

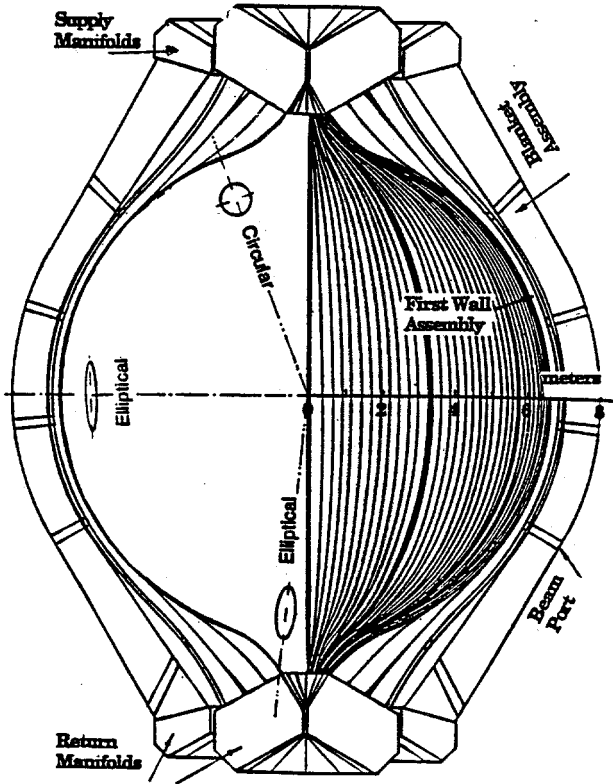


Fig. 2. Cross section of the first wall assembly showing the cross section of the first wall coolant tubing.

to bottom and have a constant cross-sectional flow area along their entire length. The coolant is a moving granular TiO_2 bed of 300-500 μm particles in helium gas at a pressure of 1.5 atm. The gas is moving upward, while the granular solid material is moving downward under gravity and hindered by the helium gas flow in the opposite direction. The velocity of the granular solid material is constant at <1.5 m/s. According to the conservation of mass principle and since this is an incompressible fluid, the flow cross-sectional area must be constant. The general shape of the SIRIUS-P chamber is spherical, therefore it is a challenging task to achieve a constant cross-sectional flow area in the first wall. An innovative idea for the coolant tube geometry along its length has been introduced (the details are discussed in [2] and [3]). The shape of the cross-sectional area of the coolant tube changes along its length to keep the cross-sectional flow area constant. At the chamber midplane the coolant tubes have an elliptical shape with the major axis along the circumferential direction. The cross-sectional area approaches a perfect circle near the top and bottom. At the top and bottom the shape of the cross-sectional area of the coolant tube is elliptical with its minor axis along the circumferential direction (Fig. 2). This insures that the velocity of the

TABLE I
Parameters of SIRIUS-P Rankine Cycle

Coolant velocity (m/s)	1.17
Helium gas pressure (atm)	1.5
At the midplane	
Bulk temperature of TiO_2 ($^\circ\text{C}$) [†]	675
Surface heat flux (W/cm^2)	151
Volumetric nuclear heating (W/cm^3)	9.575
Heat transfer coefficient ($\text{W}/\text{cm}^2\text{K}$) [†]	0.314
Coolant tube cross-section:	
a (major axis) (cm)	12.35
b (minor axis) (cm)	1.99
At the lower extremity	
Bulk temperature of TiO_2 ($^\circ\text{C}$) [†]	834
Average surface heat flux (W/cm^2) [‡]	$151 \cos 20^\circ$
Volumetric nuclear heating (W/cm^3)	9.575
Heat transfer coefficient ($\text{W}/\text{cm}^2\text{K}$) [†]	0.3102
Coolant tube cross-section:	
a (major axis) (cm)	8.25
b (minor axis) (cm)	3.0
[†] The calculations have been performed in Ref. 2.	
[‡] The tangent is inclined 20° to the normal radial direction.	

granular bed is constant at the first wall where the surface heat load from the x-rays and ion debris is very high.

II. WALL MATERIAL AND POWER CYCLE

The first wall tubes are made of 4-D weave carbon-carbon composite. The 4-D weave carbon-carbon is constructed by running fibers in three directions in one plane, 60 degrees apart, commonly called the U, V, and W plane. This results in a material with differing properties in the in-plane and perpendicular directions.

With the capability of high temperature performance of the first wall assembly, two different power cycles are considered, a conventional Rankine steam cycle (SIRIUS-PR) and a helium gas Brayton cycle (SIRIUS-PB). The first wall geometry stays the same for both cycles. The first wall thickness is 1.0 cm. In this study only the Rankine cycle will be considered. Table I shows a summary of the parameters used in this analysis.

III. THERMAL AND STRUCTURAL ANALYSIS

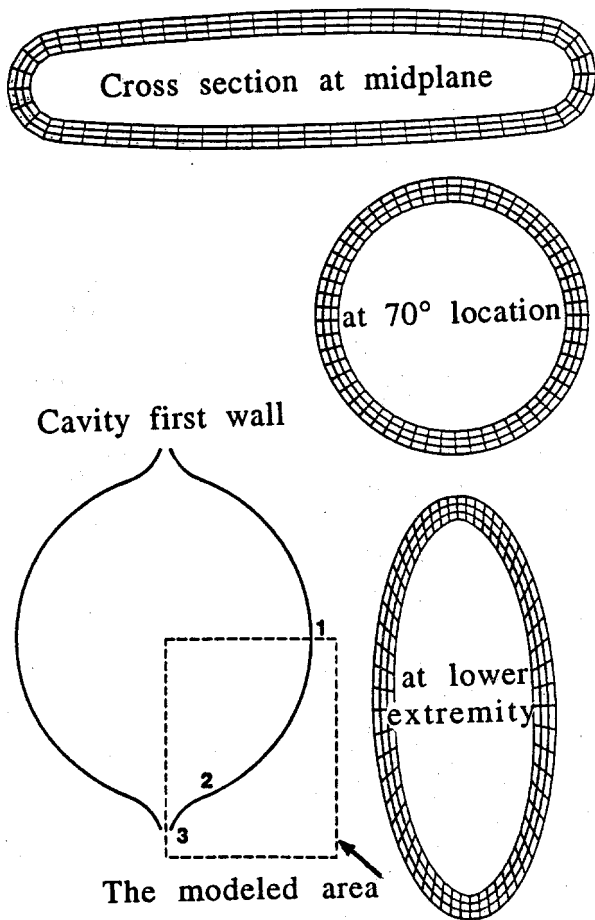


Fig. 3. A sketch of the cavity first wall showing the modeled area and the detailed shape of the coolant tube cross-sections.

The analysis uses a commercial finite element analysis code (ANSYS),¹ with complete 3-D modeling. The 3-D finite-element thermal and static stress analysis have been performed for only one of the first wall coolant channels because of the symmetry in the geometry of the first wall. Moreover, because of symmetry in the thermal and static loading, only one half (poloidally) of the coolant channel is considered in the finite-element model. Also, because of the higher coolant temperature in the lower half of the spherical chamber, we only consider the lower half of a coolant channel in the thermal and static stress calculations. Figure 3 shows a sketch of the cavity first wall identifying the area modeled. The detailed shape of the coolant tube cross-section at three key locations along the coolant channel is also shown. In the model the geometry of the cross sectional area changes constantly (keeping the internal flow area constant) from an oblong shape (with the larger dimension in the circumferential horizontal plane) at the reactor midplane to a perfect circular shape at about 70° mea-

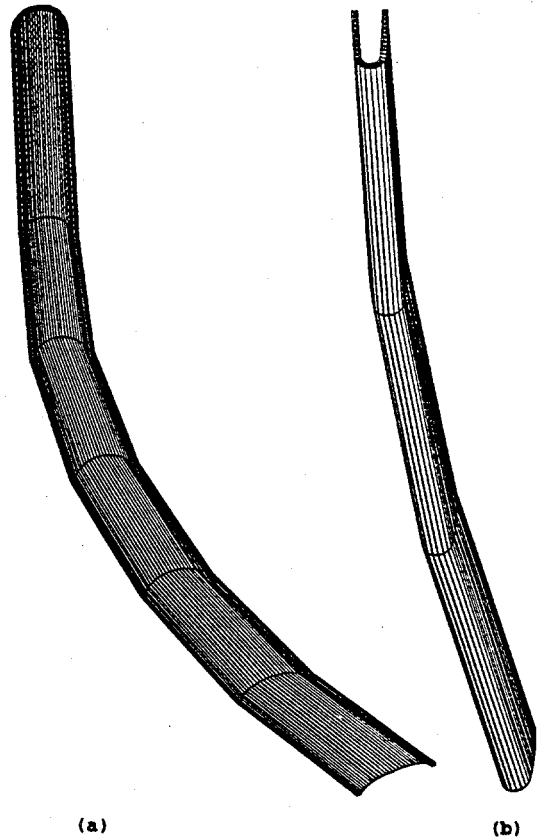


Fig. 4. (a) The first 15° of the model starting at the cavity midplane and (b) the lower part of the model.

sured from the cavity midplane and ending at the lower extremity, with an elliptical shape with its major axis in the radial direction. Figure 4 shows the first 15° of the model starting at the cavity midplane and the lower part of the model starting from the 65° location to the coolant channel lower extremity.

IV. RESULTS AND DISCUSSION

The unique shape of the coolant channel reveals quite a few interesting results. The amount of nuclear heat loading, surface and volumetric, absorbed by a single coolant channel basically depends upon several factors:

- (a) Intensity of the surface heat flux (constant in this case).
- (b) Projected area per unit height of the coolant channel; numerically it is equal to the coolant channel outer width that is constantly decreasing as we move towards the lower extremity.
- (c) Intensity of the volumetric heating per unit volume (taken as an averaged constant value in this case, because of the relatively small dimensions of the

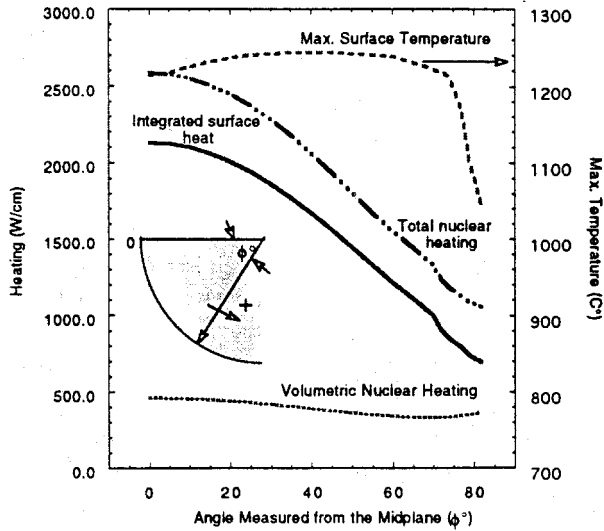


Fig. 5. The variation of the coolant bulk temperature, volumetric heating, surface heating and the total nuclear heating.

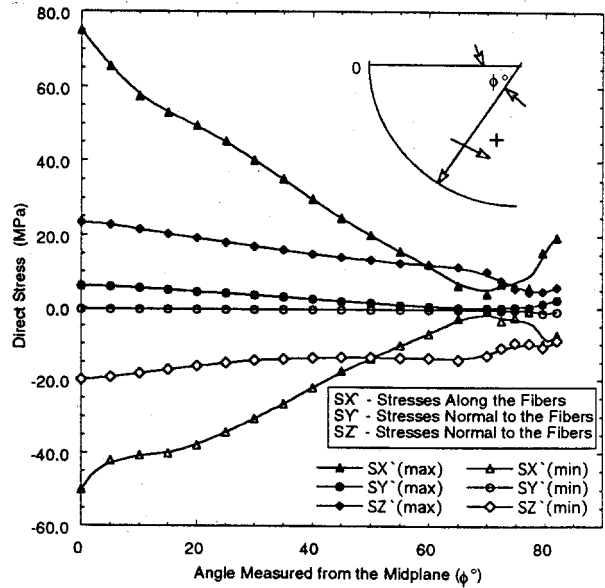


Fig. 7. The stress distribution along the fibers, normal to the fibers and along the coolant channel.

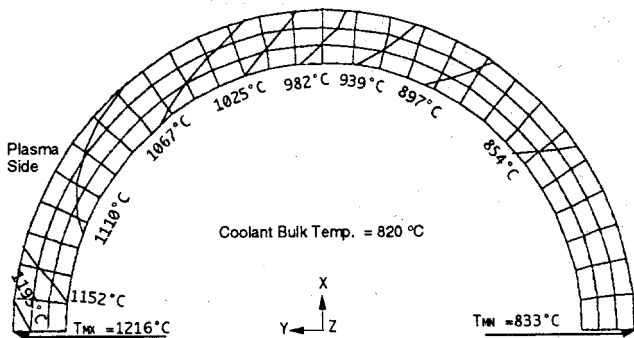


Fig. 6. The temperature distribution at 70° location.

coolant channels compared to the rather large dimensions of the reactor cavity).

(d) Volume of the coolant channel per unit height; numerically, it is equal to the coolant channel average circumference.

Figure 5 shows the variation of the coolant bulk temperature, volumetric heating, surface heating, the total nuclear heating along the coolant channel and the maximum surface temperature. Note that the minimum value of the volumetric heating per unit height occurs, as expected, at the 70° location where the coolant channel cross section is a circle (minimum volume of the coolant channel per unit height). On the same figure, the variation of the surface heat per unit height reflects its strong correlation with the coolant channel outer width. The total amount of heat carried by the coolant actually decreases as the coolant moves away from the cavity midplane to-

wards the lower extremity. This means that the wall temperature gradient must decrease, accordingly, the same way the input heat load does. In the meantime the coolant bulk temperature increases as the coolant moves away from the cavity midplane towards the lower extremity. This combination of increasing coolant bulk temperature and decreasing wall temperature gradient as the coolant moves away from the cavity midplane towards the lower extremity results in a nearly constant peak first wall temperature.

A scoping analysis has been performed to investigate the effect of the thermal stress alone. This scoping analysis confirms our findings in a previous 2-D study,^{2,3} that the thermal stresses has a minute effect on the total stresses. The results of the stress analysis are for the combined effects of thermal and static loading during steady state operation. Figure 6 shows the finite element model and the corresponding temperature distribution at 70° location. The temperature has been greatly affected by the three dimensional treatment of the problem. More than a 10% reduction in the peak steady state temperature of the first wall is encountered due to consideration of the third dimension in this analysis. Figures 7 and 8 show the stress distribution along the fibers, normal to the fibers and along the coolant channel in the ELEMENT frame of axis. These figures (7 and 8) clearly demonstrate the fact that the best cross-section is a circle; notice that the minimum stresses always occur around the 70° location where the coolant channel cross-section becomes a circle. The analysis shows

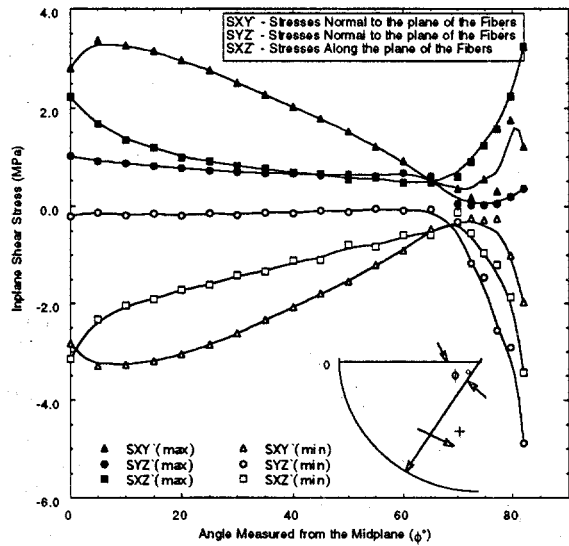


Fig. 8. The shear stress distribution along the fibers, normal to the fibers and along the coolant channel.

that the maximum tensile stress is 74.85 MPa along the fibers compared with 85.6 MPa along the fibers in the 2-D model, which reflects more than a 14% reduction in stresses along the fibers due to consideration of the third dimension. Table II shows a summary and comparison of the results of both the thermal and structural analysis as performed with 3D analysis and the original 2D analysis.⁴

VI. CONCLUSIONS

(1) All of the thermal stresses (normal to fibers, along fibers and shear stresses) are minute compared with the stresses due to static loads.

(2) It is expected that the highest stresses occur at midplane because the shape of the cross-sectional area is the flattest at that point ($a/b = 6.21$ at the midplane compared to $a/b = 2.74$ at the lower extremity).

(3) The stresses are dominated by bending due to the internal pressure of the He gas, and the stresses are proportional to the largest characteristic dimension in the cross-sectional area.

(4) It is also evident that 3D modeling for the whole coolant tube including bi-axial stresses is needed to obtain more complete results.

(5) The design is capable of withstanding the loading conditions imposed, although the effect of pulsed or partially loaded operation should be carefully examined.

ACKNOWLEDGEMENT

TABLE II

A Summary of the Results of the Structural Analysis

	3-D	2-D
Maximum temperature (°C)	1245	1398
Max. tensile stress (MPa)		
● along fibers	74.8	85.6
● normal to fibers (in the ELEMENT X-Y plane)	6.1	50.2
● along the length of the coolant tube (in the ELEMENT Z direction)	23.4	—
Max. compressive stress (MPa)		
● along fibers	50.0	57.4
● normal to fibers (in the ELEMENT X-Y plane)	32.6	44.7
● along the length of the coolant tube (in the ELEMENT Z direction)	19.9	—
Max. shearing stress, in the ELEMENT frame of axis (MPa)		
● in the X-Y plane	3.3	34.3
● in the Y-Z plane	4.9	—
● in the X-Z plane	3.4	—
Maximum displacement (cm)	0.08	0.8

Support for this work has been provided by the U. S. Department of Energy.

REFERENCES

1. Gabriel J. DeSalvo and Robert W. Gorman, "ANSYS Engineering Analysis System Users Manual," Revision 4.4, May 1989, Swanson Analysis Systems, Inc.
2. I. N. Sviatoslavsky, G. L. Kulcinski, E. A. Mogahed, et al., "SIRIUS-P, An Inertially Confined Direct Drive Laser Fusion Power Reactor," UWFDM-950, DOE/DP/10754-1, March 1993.
3. E. A. Mogahed and I. N. Sviatoslavsky, "Thermal and Structural Analysis of the First Wall in SIRIUS-P Reactor," Proc. 15th IEEE/NPSS Symp. on Fusion Engineering, Oct. 11-15, 1993, Hyannis, MA, pp. 773-779.
4. I. N. Sviatoslavsky, G. L. Kulcinski, E. A. Mogahed, et al., "A Near Symmetrically Illuminated Direct Drive Laser Fusion Power Reactor - SIRIUS-P," these proceedings.